IJE TRANSACTIONS C: Aspects Vol. 27, No. 9, (September 2014) 1457-1466

International Journal of Engineering

Journal Homepage: www.ije.ir

A Fast Immersed Boundary Fourier Pseudo-spectral Method for Simulation of the Incompressible Flows

F. Sabetghadam*[a], E. Soltani [a], H. Ghasemi [b]

[a] *Mechanical and Aerospace Engineering Faculty, Science and Research Branch,Islamic Azad University (IAU), Tehran, Iran*
[b] *Department of Maritime Engineering, Amirkabir University of Technology, Tehran, Iran*

PAPER INFO

Paper history:
Received 16 December 2013
Received in revised form16 March 2014
Accepted 17 April 2014

Keywords:
Immersed Boundary Method
Vorticity-velocity Formulation
Pseudo-Spectral Method
Moving Obstacles

ABSTRACT

The present paper is devoted to implementation of the immersed boundary technique into the Fourier pseudo-spectral solution of the vorticity-velocity formulation of the two-dimensional incompressible Navier-Stokes equations. The immersed boundary conditions are implemented via direct modification of the convection and diffusion terms, and therefore, in contrast to some other similar methods, there is not an explicit external forcing function in the present formulation. At the beginning of each time step, the solenoidal velocities (also satisfying the desired immersed boundary conditions), are obtained and fed into a conventional pseudo-spectral solver, together with a modified vorticity. The classical explicit fourth-order Runge-Kutta method is used in time integration, and the boundary conditions are set at the beginning of each sub-step, in order to increase the time accuracy. The method is employed in simulation of some different test cases, including the flow behind impulsively started circular cylinder, oscillating circular cylinder in fluid at rest and insect-like flapping wing motion. The results show accuracy and efficiency of the method.

doi:*10.5829/idosi.ije.2014.27.09c.16*

1. INTRODUCTION

Fourier pseudo-spectral solution of the voricity-based formulations of the Navier-Stokes equations (NSE) have been used widely in the two-dimensional incompressible flow simulations [1]. However, the classical implementations are limited to the regular domains with simple coordinate-coinciding boundaries and periodic boundary conditions. Now, recent advances in the immersed and embedded boundary techniques have raised hopes of extending the range of applicability of these methods to the more general domains and boundary conditions [2, 3].

To the best knowledge of authors, the immersed boundary method was applied into the vorticity-stream function formulation of the NSE by Calhoun [4, 5] for the first time. In the Calhoun's work the immersed surfaces are introduced, and the overall mass balance is satisfied, by definition of an appropriate distribution of vorticity source term. More or less similar line was followed in the work of Russell and Wang [6]. They decomposed the effects of solid wall into a no-slip condition, imposed by a boundary element method (which satisfied the overall mass balance). In the work of Linnick and Fasel[7], a higher-order compact method was used, and a source term was defined in crossing the discontinuities, which was obtained from a jumped function. Recently, Wang et al. [8] applied the direct forcing idea of Mohd-Yusof[9] into the vorticity-velocity formulation of the NSE. They added an explicit vorticity source term to the vorticity transport equation, which was obtained by taking curl of the forcing functions of momentum equations in the primitive variable form of the NSE. However, all of the above methods are based upon finite-difference or finite-volume discretization.

In the pseudo-spectral solutions, the volume penalization is one of the popular remedies, which has

*Corresponding Author's Email: fsabet@srbiau.ac.ir (F. Sabetghadam)

Please cite this article as: F. Sabetghadam, E. Soltani, H. Ghasemi, A Fast Immersed Boundary Fourier Pseudo-spectral Method for Simulation of the Incompressible Flows, International Journal of Engineering (IJE), TRANSACTIONS C: Aspects Vol. 27, No. 9, (September 2014) 1457-1466

been used several times for implementation of the no-slip condition. The method was first proposed in the primitive variables formulation of the NSE by Arquisand Caltagirone [10], and then re-formulated by Angot[11]. In the following years the method was extended to the vorticity-velocity formulation [12, 13], and used for the fixed, as well as moving boundary problems [14, 15].

A new immersed boundary method is proposed in the present paper, in which the arbitrary immersed velocity boundary conditions (including the no-slip condition), are introduced into the Fourier pseudo-spectral solution of the vorticity-velocity formulation of the NSE, without explicit addition of external forcing functions. Instead of the conventional forcing functions, the immersed boundaries are implemented by direct modification of the convection and diffusion terms of the vorticity transport equation in such a way that can be implemented to the Fourier pseudo-spectral solutions.

The paper is continued by presenting the mathematical formulations of the classical Fourier pseudo-spectral method and the suggested algorithm for imposing the immersed velocity boundary conditions. Because of its crucial role, the boundary condition setting process is presented in details, in an individual section. As our numerical experiments, the method is implemented into some fixed as well as moving boundary problems, with the surfaces which are coinciding and non-coinciding with the regular grids.

2. PROBLEM FORMULATION

The mathematical and numerical frameworks of the method are described in this section. Beginning from the classical Fourier pseudo-spectral formulation, the suggested modifications for imposing the immersed boundaries and then embedding the solution domain into the regular domain are explained.

According to Figure. 1, for a two dimensional velocity vector $\mathrm{u}=(u_1,u_2)$, defined on the regular closure $\bar{D}=(D\cup\Gamma_D)$, the dynamics of vorticity vector $w=(0,0,\ w_z=w\hat{\mathrm{e}}_z=\nabla\times\mathrm{u})$ is obtainable from time integration of the vorticity transport equation:

$$\begin{cases}\partial_t\omega+(\mathrm{u}\cdot\nabla)\omega=\nu\nabla^2\omega & \text{in} \quad D\times(0,T],\\ \omega(\mathrm{x},\ t=0)=\omega_0(\mathrm{x}) & \text{for} \quad \mathrm{x}\in\bar{D},\end{cases} \tag{1}$$

while the velocity vector u satisfies the following Poisson's problem with Dirichlet boundary conditions:

$$\begin{cases}\nabla^2\mathrm{u}=\hat{\mathrm{e}}_z\times\nabla w & \text{in} \quad D,\\ \mathrm{u}(\Gamma_D)=\mathrm{u}_{\Gamma_D}.\end{cases} \tag{2}$$

One of the advantages of the above vorticity-velocity formulation, in comparison to e.g. many primitive variable formulations, is the possibility of decomposition of the kinematics and dynamics of the flow field in each time instant. In fact, for any arbitrary distribution $w\in H^1$, the physical (divergence-free) velocity vector is obtainable from solution of Equation. (2), if the appropriate boundary conditions are imposed. As it will be seen, this issue has a vital role in construction of the physical immersed velocities in the present method.

On the other hand, to improve the efficiency of the computations, it is convenient to change the vorticity transport Equation (1) to

$$\partial_t w=\underbrace{n\nabla^2 w}_{\mathrm{L}}-\underbrace{\frac{\partial^2}{\partial x_1\partial x_2}\left(u_2^2-u_1^2\right)}_{\mathrm{N}_1}+\underbrace{\left(\frac{\partial^2}{\partial x_2^2}-\frac{\partial^2}{\partial x_1^2}\right)u_1u_2}_{\mathrm{N}_2}, \tag{3}$$

which in comparison to the classical form (1), saves one fast Fourier transform (FFT) in the pseudo-spectral algorithm. Although this formulation has been used in some other studies, to the best knowledge of the authors, in the pseudo-spectral solution of the incompressible flow, it was proposed by Chasnov[16] for the first time. The diffusion term L and the non-linear terms, N_1 and N_2, are named for the future references. In fact, the immersed velocity boundary conditions will be introduced to the solution by direct modification of these terms.

For the periodic boundary conditions, the Fourier series provides such an accurate and efficient tool which makes it worthwhile re-formulating the problem in the Fourier space. In this way, the vorticity transport Equation (3) recasts

$$\begin{cases}d_t\hat{\omega}=\underbrace{\nu\left|\mathrm{K}\right|^2\hat{\omega}}_{\hat{\mathrm{L}}}-\underbrace{k_1k_2\left(\widehat{u_1^2}-\widehat{u_2^2}\right)}_{\hat{\mathrm{N}}_1}+\underbrace{\left(k_1^2-k_2^2\right)\widehat{u_1u_2}}_{\hat{\mathrm{N}}_2},\\ \hat{\omega}(\mathrm{K},\ t=0)=\hat{\omega}_0,\end{cases} \tag{4}$$

while the Poisson problem (2) simplifies to

$$\hat{\mathrm{u}}=-i\frac{\mathrm{K}^{\perp}}{\left|\mathrm{K}\right|^2}\hat{w}; \tag{5}$$

In these equations, ($\hat{}$) stands for the quantities in the Fourier space, $\mathrm{K}=(k_1,k_2)$ is the wave number vector with the magnitude $|\mathrm{K}|^2=k_1^2+k_2^2$; while $\mathrm{K}^{\perp}=(-k_1,k_2)$ is the perpendicular wave number vector, and $i^2=-1$. Practically, in the finite dimensional calculations, the nonlinear terms $\hat{\mathrm{N}}_1$ and $\hat{\mathrm{N}}_2$ are constructed (and are de-aliased) in the physical space| the algorithm which is known (and will be referred in this paper) as the pseudo-

spectral method. Discretization in time, and time integration of the fully discretized system can be done using an appropriate time marching method. The explicit fourth-order Runge-Kutta method is used in the present work. More or less, similar formulations have been used in many efficient and accurate solvers of the periodic flow in regular domains. In the sequel we will modify Equations (4) and (5), and suggest an algorithm to use them in the flow configuration of Figure. 1.

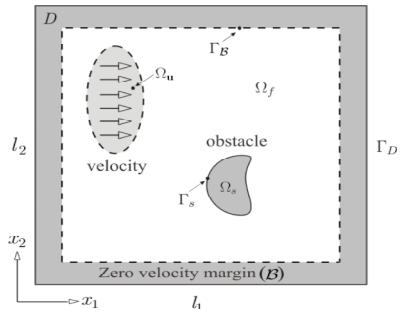

Figure 1. The flow domain Ω_f, together with fixed or moving obstacle(s), and other given-velocity regions Ω_u, are embedded in the regular solution domain D (with regular boundary Γ_D), via a zero-velocity margin B.

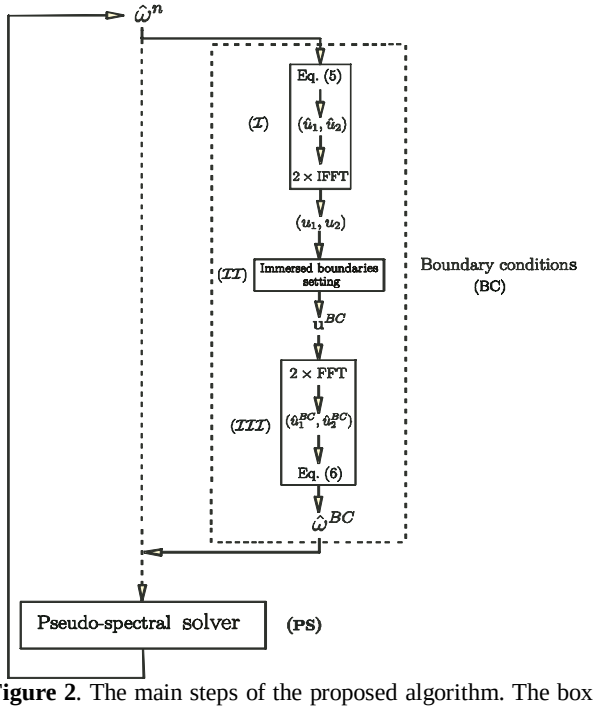

Figure 2. The main steps of the proposed algorithm. The box (PS) contains a classical Fourier pseudo-spectral solver (calculation of the right hand side of Equation. (4), solution of Equation. (5), de-aliasing, time integration. . .). Therefore, a classical Fourier pseudo-spectral solution with periodic boundary conditions can be retrieved by switching-off the boundary condition setting box, and following the dashed line.

2. 1. Implementation of the Immersed Velocity Boundary Conditions In the present method, without explicit addition of a forcing function in the right hand side of Equation. (4), the immersed surfaces are introduced by modification of the $\hat{N}_1, \hat{N}_2$ and $\hat{L}$. Particularly, it is desired to carry out these modifications such that the velocities remain solenoidal, and in a manner that the method can be implemented easily into a Fourier pseudo-spectral solver. The suggested procedure is summarized in Figure 2, in which the boundary conditions box (BC) can be more explained by the following remarks:

1. Given the vorticity field $\hat{w}^n$, from the initial condition or the last time step, the velocity vector u in the regular domain $\bar{D}$, is obtained from Equation (5)an two inverse FFTs (box (I)).

2. The velocity vector u is modified to satisfy all needed immersed velocity boundary conditions (box (II)). This conditioned velocity will be called u^{BC}. The modifications will be explained in detail in the next section. Note that u^{BC} is neither necessarily solenoidal, nor its mean value is zero at this point.

3. The conditioned vorticity w^{BC} is re-calculated from u^{BC} (that is, $w^{BC} = \nabla \times u^{BC}$), as it is shown in box (III).

There are two main reasons for this step. Firstly, the solenoidal velocities can be obtained from this conditioned vorticity in the next steps, provided that the appropriate boundary conditions are implemented; and secondly, the vorticity will be needed in the subsequent pseudo-spectral algorithm.

Although w^{BC} can be found by any method (e.g. the finite difference), to preserve the spectral accuracy, and because the vorticity in the Fourier space is needed in the subsequent steps of the pseudo-spectral algorithm, calculation in the Fourier space is suggested here. In this way:

$$\hat{w}^{BC} = i\,(k_1 \hat{u}_2^{BC} - k_2 \hat{u}_1^{BC}). \tag{6}$$

Note that, it is aimed to simulate the confined flows, and therefore, the vorticity field has zero-mean according to the Stokes theorem; the fact that legitimates the use of the above equation. Moreover, note that w^{BC} = IFFT $\{\hat{w}^{BC}\}$ is automatically defined on $\bar{D}$, it is double periodic, and it has zero mean- the properties that makes it *ready to use* for the subsequent Fourier pseudo-spectral steps.

4. The conditioned vorticity w^{BC} is fed into the classical

pseudo-spectral procedure (that is, box (**PS**) in Figure 2), in which the solenoidal velocity vector $\hat{u}_{\mathbf{Sol}}^{\mathrm{BC}}$ is calculated from:

$$\hat{u}_{\mathbf{Sol}}^{\mathrm{BC}} = -i\,\frac{\mathrm{K}^{\perp}}{|\mathrm{K}|^2}\hat{w}^{\mathrm{BC}};$$

and these velocities, in addition to the conditioned vorticity $\hat{w}^{\mathrm{BC}}$ are substituted into the modified vorticity transport equation

$$\begin{cases} d_t\hat{\omega} = \underbrace{\nu|\mathrm{K}|^2\hat{\omega}^{\mathrm{BC}}}_{\hat{\mathrm{L}}} - \underbrace{k_1k_2\left(\widehat{u_1^2-u_2^2}\right)_{\mathbf{Sol}}^{\mathrm{BC}}}_{\hat{\mathrm{N}}_1} + \\ \qquad \underbrace{\left(k_1^2-k_2^2\right)\widehat{(u_1u_2)}_{\mathbf{Sol}}^{\mathrm{BC}}}_{\hat{\mathrm{N}}_2}, \\ \hat{\omega}(\mathrm{K},\ t=0) = \hat{\omega}^{\mathrm{BC}}. \end{cases} \tag{7}$$

Time integration of the above equation yields the new vorticity field $\hat{w}^{n+1}$ which closes the algorithm loop.

An attractive feature of the above procedure is that the boundary conditions box can be added easily to a classical pseudo-spectral solver without any change in the internal structure. In fact, the box (**PS**) contains all steps of a classical pseudo-spectral solution. Moreover, note that in addition to the solid obstacles, the given immersed fluid velocities can be implemented as well.

In our numerical experiments that are presented in this paper, the fourth-order Runge-Kutta method is used for time integration, and in order to increase the time accuracy, the boundary conditions are set at the beginning of each Runge-Kutta sub-steps.

2. 2. Setting Boundary Conditions This section is devoted to a full description of the method used in setting of the immersed velocity boundary conditions (that is, modifying u into u^{BC}, mentioned in the previous subsection). The process of setting boundary condition is divided into the following sub-steps:

1. Identification of the numerical boundary points, and
2. Evaluation of the numerical boundary conditions.

The details of the above sub-steps are in orderly arranged. In what follows, we will consider one immersed body. For the multi-object problems, the method can be applied exactly in the same way. Moreover, according to Figure 3, we assume that the physical velocity boundary conditions u_{pb} are given on the physical boundary Γ_{p}, and the solution is sought in $D\setminus\left(\Omega\cup\bar{B}\right)$, and the regular domain D is overlaid by a uniform Cartesian grid (x_i, y_j).

2. 2. 1. Identification of Numerical Boundary Points In the present method, all calculations are performed on a fixed Cartesian grid. Therefore, in following of our previous work [3], we define the numerical boundary points, which play the role of Eulerian points in some fluid-solid interaction methods, which use both the Eulerian and Lagrangian points (see e.g. [17]).

Definition 1. A numerical boundary point corresponding to the given physical boundary Γ_{p}, is a point (x_i, y_j) in the Cartesian grid, if and only if

i) $(x_i, y_j)\in(\bar{\Omega}=\Omega+\Gamma_{\mathrm{p}})$

ii) C_{ij} contains at least one point from $D\setminus\bar{\Omega}$

where C_{ij} is a circle of radius $r_{ij}=\min(\Delta x,\Delta y)$, centered in (x_i, y_j).The definition is illustrated in Figure 4 (for a uniform grid), and for some more detail one can see [3].

The set of all numerical boundary points will be called the numerical boundary Γ_{N}, and that part of the Cartesian grid which is surrounded by Γ_{N} will be called the numerical immersed domain Ω_{N}.

For the fixed boundary problems, it is just needed to determine the numerical boundaries once for all computations, while for the moving boundary problems they should be updated in the beginning of each time step with the computational cost of $O(N_{\bar{\Omega}})$, where $N_{\bar{\Omega}}$ is the number of grid points in a box, contains the immersed domain $\bar{\Omega}=\Omega_{\mathrm{N}}\cup\Gamma_{\mathrm{N}}$.

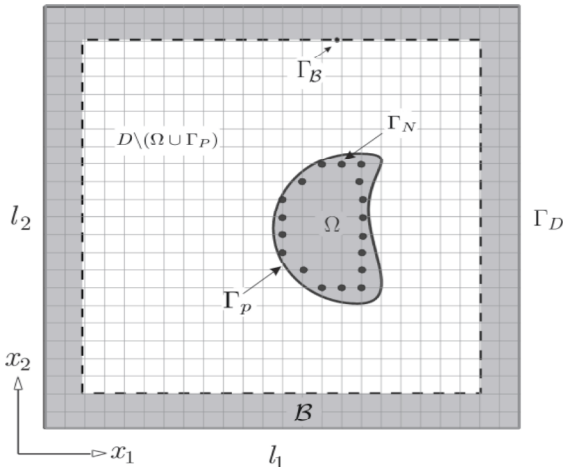

Figure 3. The numerical boundary Γ_{N} corresponding to the physical boundary Γ_{p}.The immersed boundary conditions u_{pb} are given on Γ_{p}.

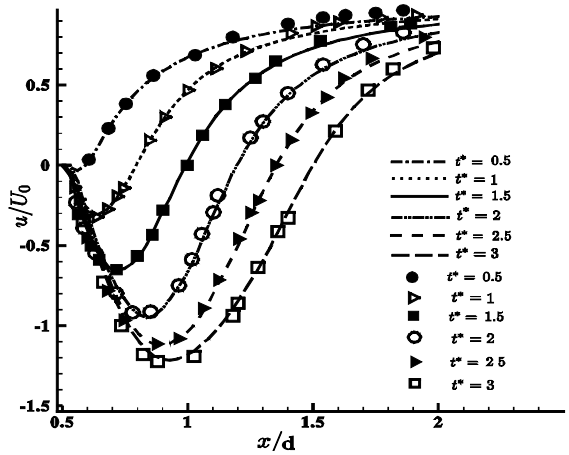

Figure 4. Time evolution of the horizontal velocity profile of impulsively started circular cylinder at Re = 550 compared with the experimental data. Lines show the results of the present method, while symbols show the experimental data [18].

2. 2. 2. Approximating the Boundary Conditions Given the numerical boundary points Γ_N, the next step is to evaluating velocities on these points (will be called u_{Γ_N}), such that the physical boundary conditions u_{pb} be satisfied approximately.

In the present work, since the method is not high-order, we suggest a simple approximation without any interpolation. Although this treatment of the boundary conditions (sometimes called staircasing[19]) is first-order, it is simple and effective. These properties might be the main reason that this method has been used in some other immersed boundary methods [2,20]. In the present formulation, the method is mostly suitable for the rigid immersed bodies (fixed and moving), however the modifications for the immersed bodies is straight forward.

The method contains the following two steps:

1) Given the numerical boundary point **nb** and the physical boundary $\Gamma_p(t)$, the physical boundary point **pb** corresponding to **nb** is obtained by intersecting $\Gamma_p$with the normal to $\Gamma_p$from **nb**(called $\hat{n}$).
2) Now, given $u_{pb}(t)$ the corresponding **unb** is calculated from:

$$u_{nb} = u_{pb} - d \otimes \omega_s,$$

where ω_s is the angular velocity vector of the immersed body. By definition, u_{Γ_N} is the set of all $\mathbf{u_{nb}}$ obtained on Γ_N.

Substitution of u_{Γ_N} for **u** results in the modified velocity vector u_{BC}, which is identical with **u** in $D \setminus \Gamma_N$, and approximately satisfies the physical boundary conditions on Γ_p.

3. NUMERICAL EXPERIMENTS

In order to assess the capabilities of the method, three test cases are analyzed in this section, including the moving boundaries, as well as given non-zero immersed velocity boundary conditions.

3. 1. Impulsively Started Circular Cylinder at Re=550 The experimental observations and the numerical simulations have revealed substantial differences between the wake structures in the low and moderate Reynolds numbers [18]. In this section Re = 550 is considered as a moderate Reynolds number. The flow in this regime is characterized by formation of an unsteady wake, which is two-dimensional at least in the early stages. Near the cylinder wall the so-called bulge phenomenon is observable which follows by a secondary vortex in the next times [18, 21, 22].

Consider a circular cylinder of diameter $\mathbf{d}$ moving with velocity $u = (U_0, 0)$ in an incompressible Newtonian quiescent fluid with kinematic viscosity u, which is confined in a square box $l_1 \times l_2 = 2p \times 2p$ on 512^2grid points. The Reynolds number is set as Re $= U_0 \mathbf{d} / u = 550$, and the ratio $l = \mathbf{d} / l_1 = 0.03$is chosen for the sake of comparisons [21, 22]. The details of the physical and geometric parameters are given in Table 1.

Time evolution ($t^* = \frac{U_0 t}{\mathbf{d}}$) of the horizontal velocity profiles on the symmetry axis behind the cylinder are compared with the experimental data in Figure 4. The figure shows a very good agreement between the results. Moreover, note that for $t^* > 2$ velocities higher U_0 are observable in places in the wake region. This is the main reason for causing bulge in the streamlines near the cylinder wall, and formation of the secondary vortex in the next times
(see [18] for a detailed discussion).

To show that the simulation was able to capture the phenomenon correctly, time history of the maximum non-dimensional velocity $-u_{max}/U_0$is compared with the experimental data in Figure 5. As one can see, the maximum velocity is increased in time monotonically, and is exceeds U_0after $t^* > 2$.

In Figure 6, time history of the non-dimensional wake length $L / \mathbf{d}$is compared with the experimental data [18]. Again a good agreement is observable. Furthermore, the nearly linear growth in the wake length is noticeable, which means an approximately

constant growth rate in the wake length. However, this growth rate has been less than the velocity of the cylinder, which is shown by the dashed line in the figure. Particularly, this means that the cylinder motion was followed by the fluid particles behind the cylinder.

TABLE 1. Geometric, physical and numerical parameters of the impulsively started circular cylinder at Re=550.

Re	$\mathbf{d}$ (m)	U_0 (m/s)	u (m^2/s)	l
550	0.4	0.05	3.63×10^{-5}	0.03

TABLE 2. The physical and numerical parameters used in the solution of the oscillating cylinder problem.

D	f	A	u	N
0.35	1	0.27852	6.12×10^{-3}	512^2

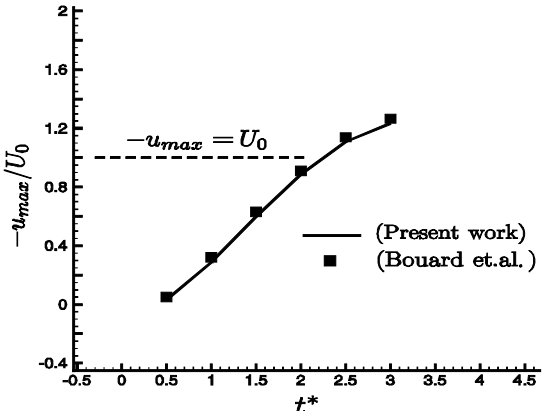

Figure 5: Time evolution of the maximum non-dimensional horizontal velocity at the symmetry axis. The horizontal velocity exceeds U_0 after $t^* > 2$.

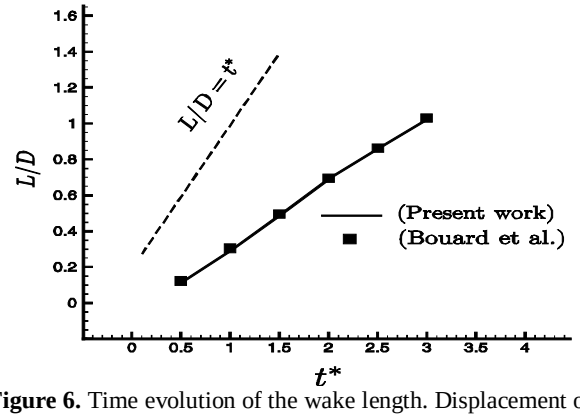

Figure 6. Time evolution of the wake length. Displacement of the cylinder center is shown by the dashed line and the wake length (the solid line) is compared with the experimental data [18]. The growth rate of the wake length is less than the cylinder center displacement.

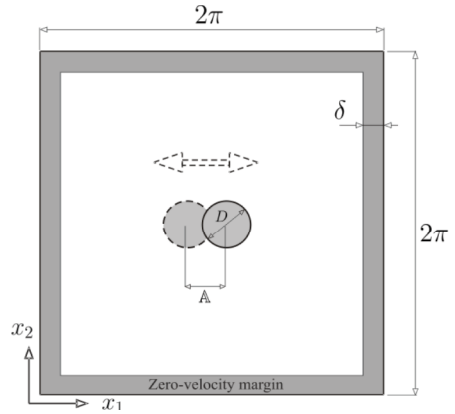

Figure 7. Geometric parameters of the oscillating circular cylinder problem.

3. 2. Oscillating Circular Cylinder in Fluid at Rest

The problem of an in-line oscillating cylinder in a quiescent fluid has been analyzed several times experimentally and numerically [23]. The geometric parameters of the fluid–solid system are illustrated in Table 2.

Previous works have revealed that [23] the flow regime is mainly under the influence of two non-dimensional parameters: the Reynolds number Re = $\frac{UD}{u}$, and the Keulegan–Carpenter number KC = $\frac{U}{fD}$; where U is the maximum velocity, f is the oscillations frequency, and D is the cylinder diameter. In the present study to facilitate assessment of the results the well-documented combination (Re,KC) = (100, 5) is considered.

A simple harmonic oscillation in the x_1 direction is exerted to the cylinder center by $x_{1c}(t) = A\sin(2pft)$, where A is the amplitude of oscillations. It can easily be shown that for this harmonic oscillation KC= $\frac{2pA}{D}$. Figure 7 illustrates the problem setup, and the main physical and numerical parameters are summarized Table 2.

More quantitative comparisons can be made by comparing the instantaneous velocity profiles, as illustrated in Figure 8. The velocities are compared with the experimental data of Dautch et al. [23]. Like other works [23, 24] for each phase angle the velocity profiles of four x_1/D sections are illustrated. As one can see, there is a general agreement between the present results and the experimental data.

3. 3. Flow Around an Insect-like Flapping Wing

In order to show the ability of the method in handling fairly complex geometries and body motions, a

combination of translating and rotating motion of an insect-like flapping wing is studied here. Understanding the unsteady characteristics of a flapping wing at high frequencies is one of the attractive problems in the field of aerodynamics of natural and man-made flyers [25]. The problem has been studied by many authors experimentally, analytically and numerically [26-28].

Here we study a simplified model for the kinematics of an insect-like flapping wing proposed by Wang [29]. In this model the wing motion comprises of two down-stroke and up-stroke translational phases, in addition to two rotational phases which change the angle of attack during the translational motions. Therefore, the flow is under the influence of the stroke amplitude, the Reynolds number and the rotational and translational speeds, in addition to the initial angle of attack [29].

In the present work, the better documented regime Re = 157 is considered [30], where the Reynolds number will be defined later.

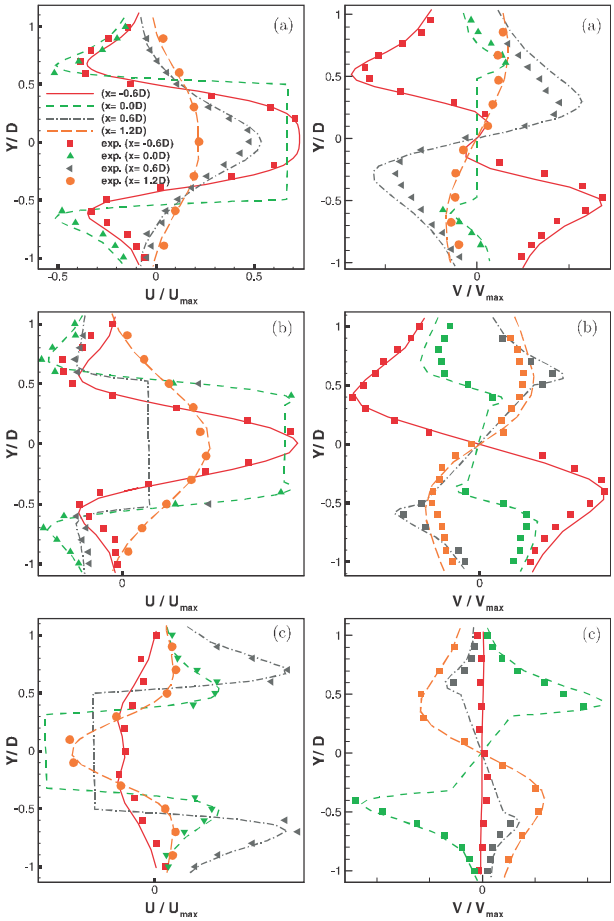

Figure 8. Comparison of the instantaneous velocity profiles for three phase angles (a): 180, (b): 210, and (c): 330. Lines show the results of the present method, while the symbols are the experimental data [23].

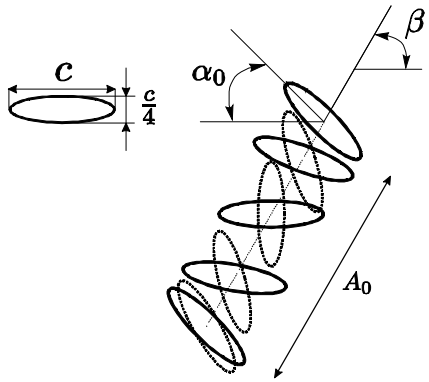

Figure 9. The geometric parameters of the insect-like flapping wing problem.

TABLE 3. The physical and geometric parameters of the insect-like flapping wing problem.

b	A_0(m)	c(m)	e	T (sec)	a_0	Re
$\frac{p}{6}$	1.25	0.5	0.25	0.0125	$\frac{p}{4}$	157

The geometric parameters are illustrated in Figure 9. The regular domain $l_1 \times l_2 = 2p \times 2p$ is chosen, and the results are presented on 512^2 grid points. The fourth-order Runge–Kutta method is used in time integration with a constant time step $\Delta t = 10^{-5}$ sec, which resulted in a stable solution. In this model an ellipse is chosen as the wing with chord c and thickness ratio e. The wing center position A(t) changes in the b direction as:

$$A(t) = \frac{A_0}{2}\left[\cos(\frac{2pt}{T}) + 1\right] \quad (8)$$

While the angle of attack $a(t)$ changes as

$$a(t) = a_0\left[1 - \sin(\frac{2pt}{T})\right].$$

In these relations T is the flappling period, and a_0 and A_0 are the initial angle of attack, and the stroke amplitude, respectively. Using the above definitions, the Reynolds number is defined as $\mathrm{Re} = \frac{pcA_0}{uT}$. The details of the physical and geometric parameters are given in Table 3. In Figure10vorticity snapshots of one flapping period are compared with the results of the second-order immersed boundary solution of Xu et al.[30].Obviously, there is a good agreement between the captured vertical structures. During the down-stroke phase, a pair of counter-rotating vortices are generated and grow (see parts (a) and (b) of Figure 10).

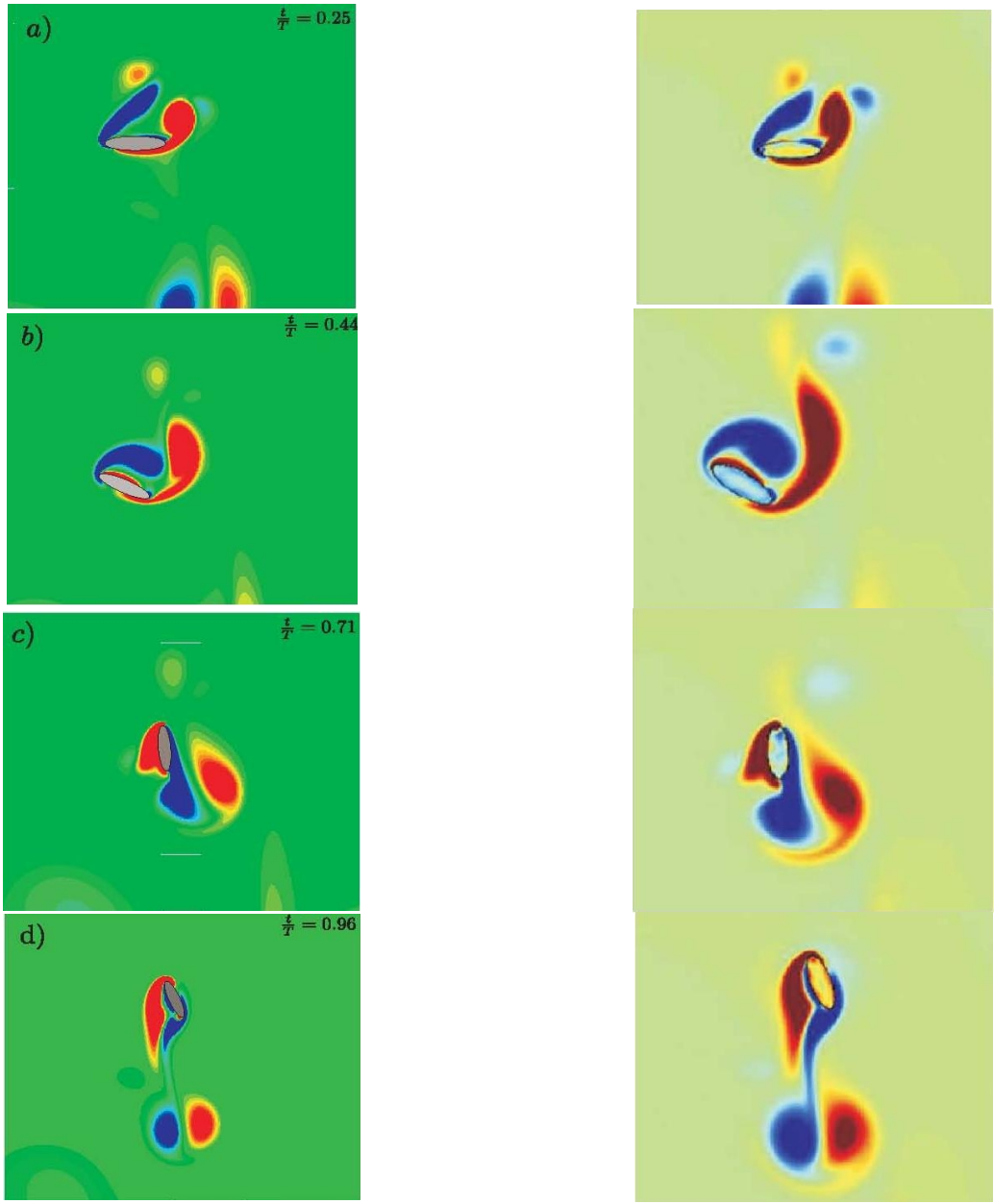

Figure 10. Distribution Vorticity snapshots of the insect-like flapping wing in the Re = 157 regime at different time instances. Left: the results of the present method. Right: the results of Xu et al. [30].

In the (d) part of Figure 10, the wing in the middle of the upstroke phase is shown. As one can see, the wing vortices separate from the wing such that the wing is no longerin the influence of these vortices at the end of this phase.

5. CONCLUSION

An immersed boundary Fourier pseudo-spectral method is proposed for the vorticity-velocity formulation of the two-dimensional incompressible NSE. The zero-mean Fourier pseudo-spectral solution is used, and therefore, the method is applicable to the confined flows, which are modeled by considering a zero velocity margin in the vicinity of the regular boundaries. Without explicit addition of external forcing functions, arbitrary Dirichlet velocity boundary conditions are implemented by direct modification of the diffusion and convection terms of the vorticity transport equation; and in this

way, it was shown that the obtained velocities are solenoidal. The immersed boundary conditions are approximated on some regular grid points (called the numerical boundary points). The method is applied to some moving boundary problems.

The impulsive started circular cylinder and oscillating circular cylinder in fluid at rest have been considered as examples of moving boundary problems. Good agreements are observed between our numerical results of unsteady features and experimental data. The method is extended to the combined translating and rotating motion of obstacles such as insect-like flapping wing motion. The dynamics of vorticity is in well agreement with predicted dynamics of other numerical simulations.

It should be noted that in contrast to some other methods, which are iterative and therefore are weakly depended on the viscosity v, our numerical solution is essentially unsteady; and therefore, its stability depends on v. Regarding this constraint, although the results are rather accurate, the method is not preferable for the steady solutions.

Moreover, the main algorithm is not restricted to the pseudo-spectral discretization method. Therefore, employing the finite–difference, or finite volume methods can be seen as other extension directions; although the rate of convergences may be different.

6. REFERENCES

1. Canuto, C., Hussaini, M., Quarteroni, A. and Zang, T., "Spectral methods in fluid dynamics (scientific computation), Springer-Verlag, New York-Heidelberg-Berlin, (1987).
2. Kolomenskiy, D. and Schneider, K., "A fourier spectral method for the navier–stokes equations with volume penalization for moving solid obstacles", ***Journal of Computational Physics***, Vol. 228, No. 16, (2009), 5687-5709.
3. Sabetghadam, F., Sharafatmandjoor, S. and Norouzi, F., "Fourier spectral embedded boundary solution of the poisson's and laplace equations with dirichlet boundary conditions", ***Journal of Computational Physics***, Vol. 228, No. 1, (2009), 55-74.
4. Calhoun, D. "A cartesian grid method for solving the stream function vorticity equations in irregular geometries", (1999).
5. Calhoun, D., "A cartesian grid method for solving the two-dimensional streamfunction-vorticity equations in irregular regions", ***Journal of Computational Physics***, Vol. 176, No. 2, (2002), 231-275.
6. Russell, D. and Jane Wang, Z., "A cartesian grid method for modeling multiple moving objects in 2d incompressible viscous flow", ***Journal of Computational Physics***, Vol. 191, No. 1, (2003), 177-205.
7. Linnick, M.N. and Fasel, H.F., "A high-order immersed interface method for simulating unsteady incompressible flows on irregular domains", ***Journal of Computational Physics***, Vol. 204, No. 1, (2005), 157-192.
8. Wang, Z., Fan, J. and Cen, K., "Immersed boundary method for the simulation of 2d viscous flow based on vorticity–velocity formulations", ***Journal of Computational Physics***, Vol. 228, No. 5, (2009), 1504-1520.
9. Mohd-Yusof, J., "Combined immersed boundary/b-splines method for simulations of flows in complex geometry", ***Annual Research Briefs, Center for Turbulence Research***, (1997).
10. Arquis, E.a.C., J.P.,, "Sur les conditions hydrodynamiques au voisinage dune interface mmilieu uide milieux poreux: Application la convection naturelle", ***Comptes Rendus de lAcademie des Sciences Paris II 299***, (1984).
11. Angot, P., Bruneau, C.-H. and Fabrie, P., "A penalization method to take into account obstacles in incompressible viscous flows", ***Numerische Mathematik***, Vol. 81, No. 4, (1999), 497-520.
12. Schneider, K., "Numerical simulation of the transient flow behaviour in chemical reactors using a penalisation method", ***Computers &Fluids***, Vol. 34, No. 10, (2005), 1223-1238.
13. Keetels, G.H., D'Ortona, U., Kramer, W., Clercx, H., Schneider, K. and Van Heijst, G., "Fourier spectral and wavelet solvers for the incompressible navier–stokes equations with volume-penalization: Convergence of a dipole–wall collision", ***Journal of Computational Physics***, Vol. 227, No. 2, (2007), 919-945.
14. Schneider, K. and Farge, M., "Numerical simulation of the transient flow behaviour in tube bundles using a volume penalization method", ***Journal of Fluids and Structures***, Vol. 20, No. 4, (2005), 555-566.
15. Clercx, H., "A spectral solver for the navier–stokes equations in the velocity–vorticity formulation for flows with two nonperiodic directions", ***Journal of Computational Physics***, Vol. 137, No. 1, (1997), 186-211.
16. Chasnov, J., "On the decay of two-dimensional homogeneous turbulence", ***Physics of Fluids***, Vol. 9, No. 1, (1997), 171-180.
17. Vanella, M. and Balaras, E., "A moving-least-squares reconstruction for embedded-boundary formulations", ***Journal of Computational Physics***, Vol. 228, No. 18, (2009), 6617-6628.
18. Bouard, R. and Coutanceau, M., "The early stage of development of the wake behind an impulsively started cylinder for $40< re< 10^4$", ***Journal of Fluid Mechanics***, Vol. 101, No. 03, (1980), 583-607.
19. Abarbanel, S., Ditkowski, A. and Yefet, A., "Bounded error schemes for the wave equation on complex domains", ***Journal of Scientific Computing***, Vol. 26, No. 1, (2006), 67-81.
20. Sugiyama, K., Ii, S., Takeuchi, S., Takagi, S. and Matsumoto, Y., "A full eulerian finite difference approach for solving fluid–structure coupling problems", ***Journal of Computational Physics***, Vol. 230, No. 3, (2011), 596-627.
21. Sanyasiraju and T.V.S.S. and Manjula, V., "Flow past an impulsively started circular cylinder using a higher-order semi-compact scheme", ***Physics Review E***, Vol. 72, No., (2005)106-110.
22. Kalita, J.C. and Ray, R.K., "A transformation-free hoc scheme for incompressible viscous flows past an impulsively started circular cylinder", ***Journal of Computational Physics***, Vol. 228, No. 14, (2009), 5207-5236.
23. Dütsch, H., Durst, F., Becker, S. and Lienhart, H., "Low-reynolds-number flow around an oscillating circular cylinder at low keulegan–carpenter numbers", ***Journal of Fluid Mechanics***, Vol. 360, (1998), 249-271.
24. Kim, D. and Choi, H., "Immersed boundary method for flow around an arbitrarily moving body", ***Journal of Computational Physics***, Vol. 212, No. 2, (2006), 662-680.
25. Shyy, W., Lian, Y., Tang, J., Viieru, D. and Liu, H., "Aerodynamics of low reynolds number flyers, Cambridge University Press New York, (2008).

26. Ellington, C.P., Van Den Berg, C., Willmott, A.P. and Thomas, A.L., "Leading-edge vortices in insect flight", (1996).
27. Pullin, D. and Wang, Z., "Unsteady forces on an accelerating plate and application to hovering insect flight", ***Journal of Fluid Mechanics***, Vol. 509, (2004), 1-21.
28. Wang, Z., "Vortex shedding and frequency selection in flapping flight", ***Journal of Fluid Mechanics***, Vol. 410, (2000), 323-341.
29. Wang, Z.J., "Two dimensional mechanism for insect hovering", ***Physical Review Letters***, Vol. 85, No. 10, (2000), 2216.
30. Xu, S. and Wang, Z.J., "An immersed interface method for simulating the interaction of a fluid with moving boundaries", ***Journal of Computational Physics***, Vol. 216, No. 2, (2006), 454-493.

A Fast Immersed Boundary Fourier Pseudo-spectral Method for Simulation of the Incompressible Flows

F. Sabetghadam[a], E. Soltani [a], H. Ghasemi [b]

[a]*Mechanical and Aerospace Engineering Faculty, Science and Research Branch,Islamic Azad University (IAU), Tehran, Iran*
[b]*Department of Maritime Engineering, Amirkabir University of Technology, Tehran, Iran*

PAPER INFO

Paper history:
Received 16 December 2013
Received in revised form16 March 2014
Accepted 17 April 2014

Keywords:
Immersed Boundary Method
Vorticity-velocity Formulation
Pseudo-Spectral Method
Moving Obstacles

چکیده

مقاله پیش‌رو به حل شبه‌طیفی فوریه معادلات ناویر-استوکس تراکم‌ناپذیر دوبعدی در فرم سرعت-تاوایی با استفاده از روش مرز مستور می‌پردازد. شرایط مرزی مستور بدون اضافه کردن تابع نیرو و از طریق اصلاح مستقیم جملات جابجایی و پخش اعمال شده‌است. در ابتدای هر گام زمانی سرعت‌های بقایی ارضاکننده شرایط مرزی مستور به‌همراه تاوایی اصلاح‌شده در معادله انتقال تاوایی اعمال می‌شوند. پیشروی زمانی با استفاده از روش صریح رانج-کوتای مرتبه چهار انجام شده است که در آن به منظور افزایش دقت، شرایط مرزی در ابتدای هر زیرگام اعمال شده‌اند. روش به مسائل مرز متحرکی شامل استوانه با حرکت ناگهانی، حرکت نوسانی استوانه در یک سیال ساکن و حرکت شبه‌بال یک حشره اعمال شده‌است. نتایج موید دقت و راندمان مناسب روش هستند.

doi:*10.5829/idosi.ije.2014.27.09c.16*